SPE 77770

# Phase Envelope Calculations for Hydrocarbon-Water Mixtures

Niels Lindeloff, Calsep, and Michael L. Michelsen, IVC-SEP, Technical University of Denmark



This paper was prepared for presentation at the SPE Annual Technical Conference and Exhibition held in San Antonio, Texas, 29 September–2 October 2002.



## Abstract

The present work describes how the pressure-temperature phase diagrams for hydrocarbon-water mixtures can be calculated. This requires a thermodynamic model that can account for the polar interactions caused by the aqueous compounds and an algorithm that can trace the two- and three-phase boundaries encountered is such systems. Models and algorithms that can handle this task are described. The paper further describes a number of examples where the methods are applied.

## Introduction

Development of HP/HT fields and the increased use of sub-sea completions and tiebacks of satellite fields result in transport of unprocessed well streams, where mixtures of hydrocarbons, water and hydrate inhibitors are transported in pipelines at high pressures. In HP/HT gas condensate fields large amounts of water can be dissolved in the hydrocarbon phases, but may separate out in the well stream during production. Due to cooling in the sub-sea environment, hydrate formation is a concern and fluid inhibitors such as methanol are often added to the well stream. The mutual solubility of hydrocarbons, water and other polars is considerable in such systems. Furthermore, both oil and condensate systems may exhibit behavior where three phases are present at low temperatures.

Being able to properly simulate this type of systems puts some additional requirements on the simulation model, both in terms of thermodynamic model and calculation algorithms. Operating conditions to be accounted for range from bottomhole pressures and temperatures, which can be in the order of 200 °C/400 °F and 1000 bar/15,000 psi, and down to deepwater seabed temperatures in the order of 0°C/ 32°F and low pressure. The two-parameter Equations of State such as the Soave-Redlich-Kwong (SRK)[1] and the Peng-Robinson (PR)[2] models have gained widespread acceptance in the petroleum industry for their ability to correlate hydrocarbon system behavior up to high pressures. The limitations of the classical formulation of the cubic EoS are well understood, and include failure to correctly handle polar systems where local composition effects dominate, and problems in correlating system behavior over a large temperature range. These problems have been addressed previously in literature. A brief review will be given of the approaches taken here to remedy the mentioned shortcomings. In terms of algorithms, two fundamental types are required. These are a multiphase flash[3] which have been described elsewhere, and a phase envelope algorithm which can trace boundaries between the different regions of the phase diagram. The construction of an envelope for two-phase hydrocarbon systems is known technology and an account for how this is done can be found in literature[4]. The problem is greatly complicated by the introduction of an aqueous phase or a third hydrocarbon phase, and the concepts applied to handle this complexity is the topic of the present paper.

## Thermodynamic modeling approach

In the following, a brief review of the thermodynamic modeling concepts applied in the present work will be given. More detailed descriptions can be found in the references. The calculations in the present work were performed using the SRK EoS with temperature dependent Peneloux volume shifts, but the following approaches apply in principle to any two parameter EoS.

The classical quadratic mixing rule for the equation of state a-parameter is shown in Eqn. 1.

$$a = \sum_{i=1}^{N} \sum_{j=1}^{N} z_i z_j a_{ij} \qquad (1)$$

where $a_{ij}$ is defined in Eqn. 2

$$a_{ij} = \left(a_i a_j\right)^{1/2} \left(1 - k_{ij}\right) \qquad (2)$$

In these equations, $a_i$ and $a_j$ are the pure component a-parameters for the corresponding species, $z_i$ and $z_j$ the corresponding mole fractions and $k_{ij}$ the binary interaction coefficient. $N$ is the number of components in the mixture. The

classical mixing rule with a single binary interaction parameter per pair is well suited for the description of mixtures that exhibit only modest deviation from ideal solution behavior. Systems like water/hydrocarbon mixtures where immiscible liquid phases may form, cannot be modeled in a satisfactory manner with this approach. If the interaction coefficient between water and a hydrocarbon is adjusted to provide a satisfactory description of the water solubility in the hydrocarbon phase, the hydrocarbon solubility in the aqueous phase is mispredicted by orders of magnitude.

A satisfactory description of the mutual solubilities is possible with the use of local composition based excess Gibbs energy models, such as UNIQUAC[5] or NRTL[6]. The excess Gibbs energy models as such, however, can only be applied for a liquid phase at low pressure. They cannot account for the effect of pressure, and their use requires a separate model for the vapor phase. Fortunately, Huron and Vidal[7] have derived a procedure that enables incorporating any excess Gibbs energy model expression into an equation of state like SRK. Equally important they described a specific variant of the NRTL-model, which can be parameterized in such a manner that the conventional mixing rule, Eqns. (1,2) is recovered. This implies that a much improved representation of the interaction between non-polar hydrocarbons and polar components like water and methanol is possible, while preserving the existing good representation of the classical mixing rule for hydrocarbon-hydrocarbon interactions. Application of this concept for hydrocarbon-water systems was described by Pedersen et al.[8] and will be briefly reviewed here for the SRK equation in combination with the NRTL model.

The Huron and Vidal a-parameter mixing rule takes the following form

$$a = b\left(\sum_{i=1}^{N}\left(z_i \frac{a_i}{b_i}\right) - \frac{G^E_\infty}{\ln 2}\right) \qquad \textbf{(3)}$$

In this equation, $z$ is the mole fraction, $a$ and $b$ the equation of state parameters, $i$ the component index and $G^E{}_\infty$ the excess Gibbs energy at infinite pressure. $G^E{}_\infty$ in this case comes from a modified NRTL mixing rule[7] as shown in Equation 4.

$$\frac{G^E_\infty}{RT} = \sum_{i=1}^{N} z_i \frac{\sum_{j=1}^{N} \tau_{ji} b_j z_j \exp\left(-\alpha_{ji}\tau_{ji}\right)}{\sum_{k=1}^{N} b_k z_k \exp\left(-\alpha_{ki}\tau_{ki}\right)} \qquad \textbf{(4)}$$

$\alpha_{ij}$ is a non-randomness parameter to account for the local composition effects (local mole fraction may differ from overall mole fraction), $\alpha_{ij} = 0$ corresponds to a completely random mixture. The parameter $\tau_{ij}$ accounts for the interaction between molecules via the following expression

$$\tau_{ji} = \frac{g_{ji} - g_{ii}}{RT} \qquad \textbf{(5)}$$

where $g_{ji}$ is an energy parameter characteristic of the j-i interaction. A very useful feature of the Huron-Vidal mixing rule is that it reduces to the classical quadratic mixing rule from Equation 1 and 2 when the $\alpha$ and $g$ parameters are selected as follows

$$\alpha_{ij} = 0 \qquad \textbf{(6)}$$

$$g_{ii} = -\frac{a_i}{b_i}\ln 2 \qquad \textbf{(7)}$$

$$g_{ji} = -2\frac{\sqrt{b_i b_j}}{b_i + b_j}\sqrt{g_{ii} g_{jj}}\left(1 - k_{ij}\right) \qquad \textbf{(8)}$$

where $k_{ij}$ is the binary interaction parameter from the classical a-parameter mixing rule discussed above. This means that this model may be applied for mixtures of hydrocarbons and polar compounds alike, allowing for a proper description of the behavior of the polar compounds while maintaining the classical model for the hydrocarbon compounds. To ensure good representation of pure component vapor pressures for the polars, the Mathias-Copeman[9] temperature dependence of the a-parameter is used for these compounds.

Pedersen et al.[10] found that while a given set of α and $g$ parameters perform well in a 50 °C temperature range, the predictions deteriorate at temperatures further away from the conditions where the parameters were estimated. To improve predictions, the g-parameters are made temperature dependent.

$$g_{ji} - g_{ii} = (g_{ji} - g_{ii})' + T\left(g_{ji} - g_{ii}\right)'' \qquad \textbf{(9)}$$

where $(g_{ji}-g_{ii})'$ and $(g_{ji}-g_{ii})''$ are temperature independent parameters.

## Phase Envelope Algorithm

Pedersen et al.[8] have previously presented an algorithm for calculating phase boundaries in 3-phase mixtures containing hydrocarbons and aqueous components like water, alcohols and glycols. The scope of this algorithm was more limited, as the incipient phase had to be a hydrocarbon phase, and only the temperature range from about 250 to about 450 K was considered.

The present algorithm, in contrast, is capable of automatic generation of the entire phase diagram, i.e. the lines that separate the regions in the P,T-plane where 1, 2 and 3 phases, respectively, are present. A generic PT phase diagram is shown in Figure 1. The key steps in the new algorithm are

i) Tracing the dewline segments that separate the single phase region from the two-phase region. (Lines I and II in Figure 1)

ii) Determining the 3-phase points on the dewline. These are the points where the overall composition is at equilibrium with two incipient phases.

iii) Tracing the phase boundaries that separate the 2-phase region from the 3-phase region. (Lines III and IV in Figure 1) These phase boundaries emerge from the 3-phase points or exist as isolated lines.

Let the overall composition of the *N*-component mixture be ***z***. Points on the dewline satisfy the following set of equations.

$$\ln w_i + \ln \varphi_i(\mathbf{w}) - \ln z_i - \ln \varphi_i(\mathbf{z}) = 0, \quad i = 1,2,...,N \qquad \textbf{(10)}$$

$$\sum_{i=1}^{N} w_i - 1 = 0 \qquad \textbf{(11)}$$

where ***w*** is the composition of the incipient phase. An additional requirement is that the mixture is stable. Stability is investigated by minimizing the tangent plane distance[11]. The minima are found at compositions ***y*** where

$$\ln y_i + \ln \varphi_i(\mathbf{y}) - \ln z_i - \ln \varphi_i(\mathbf{z}) = k, \qquad i = 1,2,...,N \qquad \textbf{(12)}$$

$$\sum_{i=1}^{N} y_i - 1 = 0 \qquad \textbf{(13)}$$

and stability requires that *k* is non-negative at all solutions to (12).

We initiate the calculation of the dewline by calculating the dewpoint at atmospheric pressure. Initial estimates are generated in a similar manner as in Pedersen et al[8]; for the vapor phase we take $\varphi_i^v = 1$, for a hydrocarbon component in a hydrocarbon liquid or for an aqueous component in a water rich liquid $\ln \varphi_i^l = \ln \varphi_i^{Wilson}$ is used, and finally for aqueous components in a hydrocarbon liquid or hydrocarbon components in an aqueous liquid, $\ln \varphi_i^l = \ln \varphi_i^{Wilson} + 10$. Here the Wilson K-factor approximation is utilized,

$$\ln \varphi_i^{Wilson} = \ln\left(\frac{P_{ci}}{P}\right) + 5.373(1+\omega_i)\left(1 - \frac{T_{ci}}{T}\right) \qquad \textbf{(14)}$$

with $T_{ci}$ being the critical temperature, $P_{ci}$ the critical pressure and $\omega_i$ the acentric factor for the i'th component. This gives two sets of liquid phase fugacities, $\ln \varphi_i^{l,hc}(T,P)$ and $\ln \varphi_i^{l,aq}(T,P)$ that apply for a hydrocarbon phase and an aqueous phase, respectively.

Substituting the above expressions in eqn. (10) results in

$$\sum_{i=1}^{N} x_i = \sum_{i=1}^{N} \frac{z_i}{\varphi_i^l(T,P)} = 1 \qquad \textbf{(15)}$$

which can be solved for the temperature. The choice of a hydrocarbon liquid or an aqueous liquid will give different results. The one yielding the higher temperature is chosen. The full set of equations (10,11) are subsequently solved by a partial Newton's method, where the composition dependence of the fugacity coefficients is not taken into account. Finally the converged solution is tested for stability as follows: A trial phase composition is generated from

$$X_i = z_i \frac{\varphi_i(\mathbf{z})}{\varphi_i^{l*}}, \quad x_i = \frac{X_i}{\sum_j X_j} \qquad \textbf{(16)}$$

where $\varphi_i^{l*}$ represents the Wilson-based fugacities for the phase type that was not used in the high temperature solution of eqn. (15). The stability equations are converged by successive substitution [11] and, if necessary, Newton's method. In case the solution determined initially is unstable, the phase type for the initial liquid is changed, and a revised (higher) dewpoint temperature is calculated.

Subsequent calculation of points on the dewline at higher pressures are performed as described by Michelsen[4]. This results in the construction of line I in Figure 1. Each calculated point is checked for stability as described above. If instability is discovered the next step is to determine the corresponding 3-phase point, where the overall composition ***z*** is at equilibrium with two incipient phases. The equations that must be satisfied at a 3-phase point are

$$\begin{aligned} &\ln w_i + \ln \varphi_i(\mathbf{w}) - \ln z_i - \ln \varphi_i(\mathbf{z}) = 0 \\ &\ln x_i + \ln \varphi_i(\mathbf{x}) - \ln z_i - \ln \varphi_i(\mathbf{z}) = 0 \\ &\sum_{i=1}^{N} x_i - 1 = 0 \\ &\sum_{i=1}^{N} w_i - 1 = 0 \end{aligned} \qquad \textbf{(17)}$$

It is first attempted to solve these by a partial Newton's method where again the partial composition derivatives of the fugacity coefficients are disregarded. Initial estimates of the phase compositions are available from the dewpoint calculations (***w***) or the stability analysis (***x***). Final convergence is obtained by means of a full Newton's method.

The phase compositions, temperature and pressure at the 3-phase points are recorded for later use, and the calculation of the dewline is continued after switching the phase types for the incipient phases. Thus, if the initial branch of the dewline had a hydrocarbon liquid as the incipient phase we continue after the 3-phase point with an aqueous phase as the incipient, and for this branch, the hydrocarbon phase Wilson-expressions are used to initiate the stability analysis. This corresponds to line II in Figure 1. In case instability is detected again, the new 3-phase point is calculated and the construction continued. The dewline terminates when the pressure exceeds a specified upper limit. Cases where no 3-phase point, a single point or 2 points are found, are common.

The next step is to trace the 3-phase phase boundaries that initiate from the 3-phase points. Each 3-phase point 'generates' two 3-phase lines, one with an incipient hydrocarbon phase (line IV) and one with an incipient aqueous phase (line III). It is convenient to use the incipient phase as the reference phase for the equilibrium factors. Let the incipient phase composition be ***w*** and that of the other phases ***x*** and ***y***, and let $\boldsymbol{\beta}$ be the fraction of total moles in the **y** phase. Defining equilibrium factors,

$$K_{ix} = \frac{x_i}{w_i}, \quad K_{iy} = \frac{y_i}{w_i} \tag{18}$$

the overall material balance,

$$z_i = \beta y_i + (1-\beta)x_i \tag{19}$$

allows all phase compositions to be expressed in terms of these variables, i.e.

$$w_i = \frac{z_i}{\beta K_{iy} + (1-\beta)K_{ix}}, \quad x_i = K_{ix} w_i, \quad y_i = K_{iy} w_i \tag{20}$$

The equations that apply along the phase boundary are

$$\begin{aligned} &\ln K_{iy} + \ln \varphi_i(\mathbf{y}) - \ln \varphi_i(\mathbf{w}) = 0 \\ &\ln K_{ix} + \ln \varphi_i(\mathbf{x}) - \ln \varphi_i(\mathbf{w}) = 0 \\ &\sum_i w_i - 1 = 0, \quad \sum_i (y_i - x_i) = 0 \end{aligned} \tag{21}$$

together with a specification equation that specifies the value of *T, P,* $\boldsymbol{\beta}$ or one of the *K*-factors.

As independent variables we use the logarithm of the *K*-factors, *T* and *P*, and the phase fraction . The sets of equations are solved by Newton's method, and the extrapolation method described by Michelsen[4] for 2-phase phase boundaries are used for generating initial estimates.

The initial point on the 3-phase line is the 3-phase point, corresponding to $\boldsymbol{\beta} = 1$, $\boldsymbol{y} = \boldsymbol{z}$ and the choice of incipient phase decides which of the branches to follow. The tracing of the 3-phase line is terminated if we return to a 3-phase point, or if an upper or a lower prescribed value of the pressure is exceeded.

Finally, in case no 3-phase point is found on the dewline, a search for an inner, isolated 3-phase region as described earlier by Pedersen et al.[8] is carried out.

The procedure of Michelsen[4] in addition enables locating critical points on the dewline and on the 3-phase phase boundaries. For critical points on a 3-phase boundary the incipient phase will always be one of the critical phases. We may therefore check for passing a critical point by a sign change in the *log K* for either the $\boldsymbol{x}$- or the $\boldsymbol{y}$-phase.

These phases cannot become mutually critical except in the rare coincidence of a critical 3-phase point. The stepsize selection procedure of Michelsen is designed to place the specifications at a 'safe' distance from the critical point, since the set of equations become very ill-conditioned in the critical region. If specifications very close to the critical point are attempted it may not be possible to converge the set of equations, (21), since round-off errors corrupt the calculated Jacobian.

One situation that cannot be handled by appropriate step selection is that of a near critical 3-phase point. In rare cases it has been impossible to converge Eqns. (17) since one of the phase pairs was almost critical. The solution we have used to overcome this problem is to perform the calculations in quadruple precision, if this is deemed necessary. Such calculations are extremely costly, the performance penalty being about a factor of 20. Therefore the switch to quadruple precision is only made near a critical point. We define the criterion for near criticality as when the K-factors for one phase all fall in the range from 0.9 to 1.1.

## Examples

In the following, we present a number of examples illustrating the different types of phase diagrams that we have encountered for hydrocarbon-water mixtures. The examples have been selected with a view to obtaining behavior that tests the algorithm to the limits, but are nonetheless compositions that could be encountered at different stages in a production scenario. The model have been verified against data at relevant operating conditions[8,10], but it should be noted that no data are available to verify the model at the very high temperatures that are also included in the phase diagrams shown.

The uncharacterized compositions of the fluids considered are given in Table 1. In all cases the fluids were characterized following the principles of the Pedersen[12] method, and calculations were carried out using the SRK-Peneloux EoS with the Huron and Vidal mixing rule implemented as described previously in this work.

The first example, Fluid A, concerns a dry gas with a low water content, 500 ppm (wt) of water. The resulting phase diagram has been plotted in Figure 2. In this case the water dewline separates the single-phase vapor region from a two-phase vapor-liquid water region. At lower temperatures, the hydrocarbon dewline separates the two-phase region from a three-phase region in which vapor, liquid hydrocarbon and liquid water phases coexist. The algorithm in this case starts by tracing the water dewline. Since no three-phase points are encountered on this line the search for an inner three-phase line is used to locate the hydrocarbon dewline.

The second example, Fluid B, is a gas condensate. The waterfree hydrocarbon phase envelope for this fluid is shown in Figure 3. Adding water to the system, corresponding to an 8 % watercut at stock tank conditions, leads to a phase diagram as shown in Figure 4. Lines marked W are phase boundaries where the incipient phase is aqueous. Boundaries where the incipient phase is carbon-rich are marked H. In Figure 4, the water dewline crosses the hydrocarbon dewline, and consequently, when tracing the first two-phase dewline the algorithm locates a three-phase point, marked by a triangle on the figure. The three-phase point in effect defines the starting point for locating the remaining three curves. Compared to the waterfree phase envelope, the presence of the water mainly affects the three-phase hydrocarbon dewline. This effect can become very pronounced at higher watercuts, as is illustrated in Figure 5. In Figure 5, the mutual solubility of water and hydrocarbons leads to a very significant deformation of the region where two hydrocarbon phases are present. This effect

is most dramatic at very high temperatures but will also affect the curves at temperatures, which are representative for normal operating conditions. The presence of methanol will further have a large effect on the mutual solubilities of hydrocarbons and aqueous compounds. This is illustrated in Figure 6, where the aqueous phase contains 50 wt% methanol, corresponding to a 60% watercut at stock tank conditions. In this case, the two-phase hydrocarbon dewline denoted 2-H separates the single phase vapor region from a vapor-hydrocarbon liquid region. Moving towards lower temperature at pressures below the critical point, a three-phase water dewline (3-W) is encountered which ends in a critical point. Moving past the critical point a three-phase hydrocarbon dewline denoted 3-H borders the other side of the three-phase region. Above the 3-H line, vapor coexists with a liquid water phase.The effect of having an aqueous phase with a significant methanol content present is further illustrated for Fluid C in Figure 7. In this case the fluid is mixed with water and methanol in a proportion corresponding to a 60% watercut at stock tank conditions. Approximately 30 wt% methanol was added to the water. In Figure 7, the phase diagram for this mixture is compared to the phase diagram for the waterfree Fluid C, illustrated by the dotted line. The plot clearly demonstrates that a dramatic effect is to be expected both for the hydrocarbon dewline as well as for the hydrocarbon bubble line in such a system.

A final example will serve to illustrate the situation where more than one three-phase point is encountered. Figure 8 shows the phase diagram for Fluid D mixed with water corresponding to a 75% watercut at stock tank conditions. Fluid D is a gas condensate. Part of the features discussed for this phase diagram occurs outside the temperature range that is relevant for normal operating conditions. They are nonetheless of interest since the stepwise nature of the algorithm makes it necessary to consider these parts of the phase diagram as well. The algorithm starts by tracing the two-phase dewlines, which in turn leads to the location of the two three phase points. Subsequently, the three-phase lines are traced. The lines emerging from the three-phase point with the lower pressure has two separate branches whereas the lines from the high pressure three-phase point forms a closed curve. An interesting feature for this fluid system is the deformation of the hydrocarbon dewline around the 'low-pressure' three-phase point. This is caused by an increase in solubility of the hydrocarbons around the three-phase point, where for Fluid B a decrease in solubility was observed. The closed three-phase area at high temperature and pressure is a region where a hydrocarbon liquid is forming in addition to the vapor and aqueous phases already present.

## Conclusions

An algorithm for automatic calculation of phase boundaries in three-phase systems with a hydrocarbon liquid and an aqueous liquid has been developed. In contrast to earlier algorithms the complete phase diagram, including two-phase and multi-phase critical points, is generated without user intervention.

The model calculations indicate that mixtures of interest for the petroleum industry can exhibit complex behavior, including multiple three-phase regions. The complex behavior observed for some of these systems emphasize the need for thermodynamic models that can properly account for the hydrocarbon-water interactions.

## References

1. Soave, G. (1972): Chem. Eng. Sci., 27, 1197-1203.
2. Peng, Y. and Robinson, D.B. (1976): Ind. Eng. Chem. Fundam., 15, 59-64
3. Michelsen, M.L. (1994): Comp. Chem. Eng., 18, 545.
4. Michelsen, M.L. (1980): Fluid Phase Equilibria, 4, 1-10
5. Abrams, D. and Prausnitz, J.M. (1975): AIChE J., 21, 116-122
6. Renon, H. and Prausnitz, J.M. (1968): AIChE J., 14, 135-144
7. Huron, M.J. and Vidal, J. (1979): Fluid Phase Equilibria,3,255-271
8. Pedersen, K.S., Michelsen, M.L. and Fredheim, A.O., (1996), Fluid Phase Equilibria 126, 13-28
9. Mathias, P.M. and Copeman, T.W. (1983), Fluid Phase Equilibria, 13, 91-108
10. Pedersen, K.S., Milter, J. and Rasmussen, C.P. (2001) Fluid Phase Equilibria, 189, 85-97
11. Michelsen, M.L. (1982, a,b) Fluid Phase Equilibria,9,1-20, 21-40.
12. Pedersen, K.S., Blilie, A. and Meisingset, K.K. (1992). Ind. Eng. Chem. Res., 31, 924-932.

## Nomenclature

$a$ = *Mixture parameter of cubic EOS*
$a_i$ = *Pure component parameter of cubic EOS*
$a_{ij}$ = *Binary mixture parameter of cubic EOS*
$b$ = *Mixture volume parameter of cubic EOS*
$b_i$ = *Pure component volume parameter of cubic EOS*
$G^E$ = *Molar excess Gibbs energy*
$g_{ji}$ = *Interaction energy between species j and i*
$k_{ij}$ = *Binary interaction coefficient*
$K_i$ = *Equilibrium factor, eqn. (18)*
$N$ = *No. of components in mixture*
$M$ = *Molecular weight (g/mol)*
$P$ = *Pressure (Bar)*
$R$ = *Gas constant*
$T$ = *Temperature (K)*
$w_i$ = *w-phase mole fraction of component* i
$x_i$ = *x-phase mole fraction of component* i
$y_i$ = *y-phase mole fraction of component* i
$z_i$ = *Overall mole fraction of component* i

***Greek***

$\alpha_{ij}$ = *Non-randomness parameter*
$\beta$ = *Vapour fraction*
$\varphi_i$ = *Fugacity coefficient, component* i
$\rho$ = *Density (g/cm$^3$)*
$\tau_{ji}$ = *Parameter in NRTL-equation, eqn. (5)*
$\omega_i$ = *Acentric factor, component* i

| | Fluid A | Fluid B | Fluid C | Fluid D |
|---|---|---|---|---|
| $N_2$ | 0.50 | 0.00 | 1.12 | 0.30 |
| $CO_2$ | 0.34 | 2.79 | 1.00 | 3.40 |
| $C_1$ | 0.84 | 71.51 | 47.00 | 71.70 |
| $C_2$ | 89.95 | 5.77 | 4.00 | 8.00 |
| $C_3$ | 5.17 | 4.10 | 2.77 | 3.80 |
| $iC_4$ | 2.04 | 1.32 | 0.51 | 0.80 |
| $nC_4$ | 0.36 | 1.60 | 2.15 | 1.50 |
| $iC_5$ | 0.55 | 0.82 | 0.84 | 0.70 |
| $nC_5$ | 0.14 | 0.64 | 1.15 | 0.80 |
| $C_6$ | 0.10 | 1.05 | 1.84 | 1.00 |
| $C_{7+}$ | 0.01 | 10.40 | 37.58 | 8.00 |
| *$M_{7+}$* | *n/a* | *191* | *251* | *156* |
| *$\rho_{7+}$* | *n/a* | *0.82* | *0.88* | *0.815* |

**Table 1: Compositions of the four fluids.**

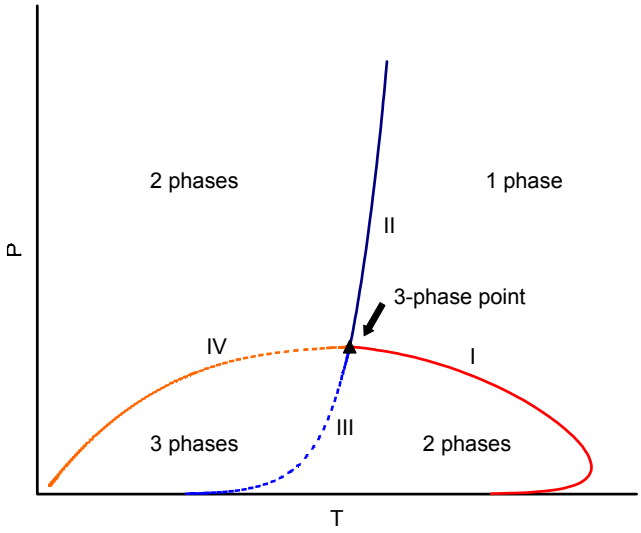


**Figure 1: Generic PT phase diagram for a hc-water system**

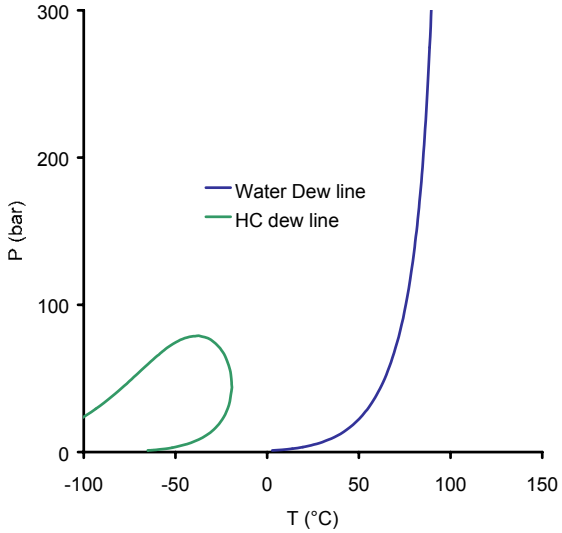


**Figure 2: Phase diagram for Fluid A with 500 ppm water**

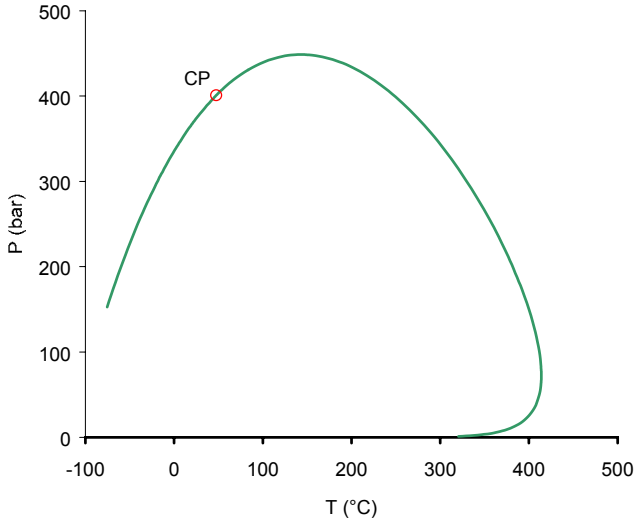


**Figure 3: Phase envelope for waterfree condensate, Fluid B**

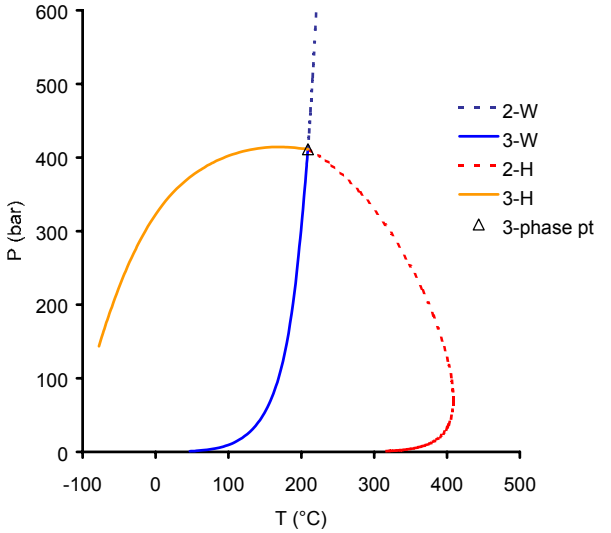


**Figure 4: Phase diagram Fluid B with 8 % watercut.**

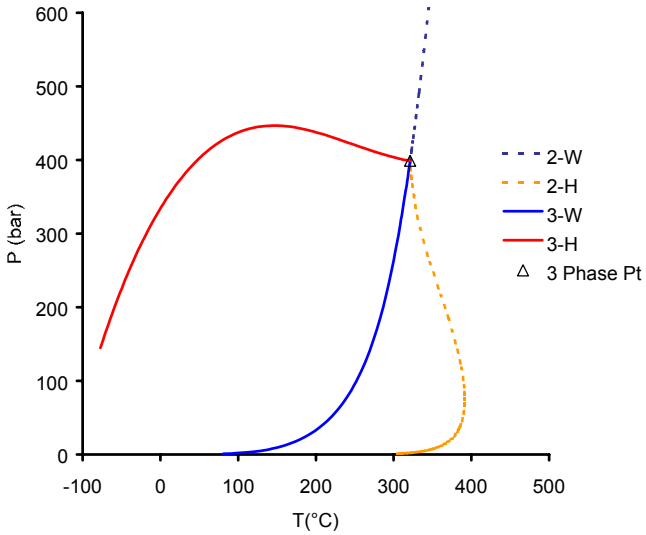


**Figure 5: Fluid B with 40% water cut.**

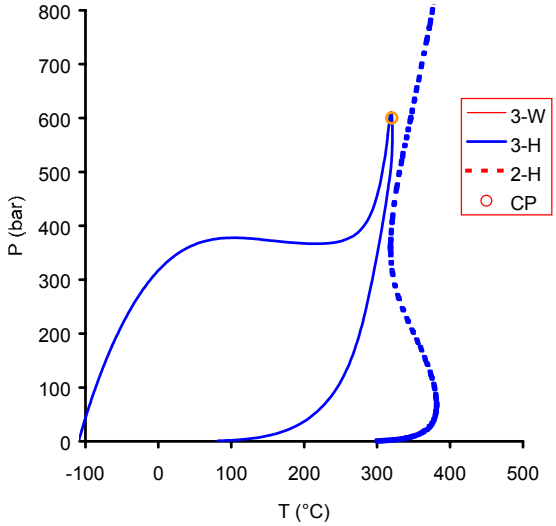


**Figure 6: Fluid B with water and MeOH corresponding to a 60% water cut.**

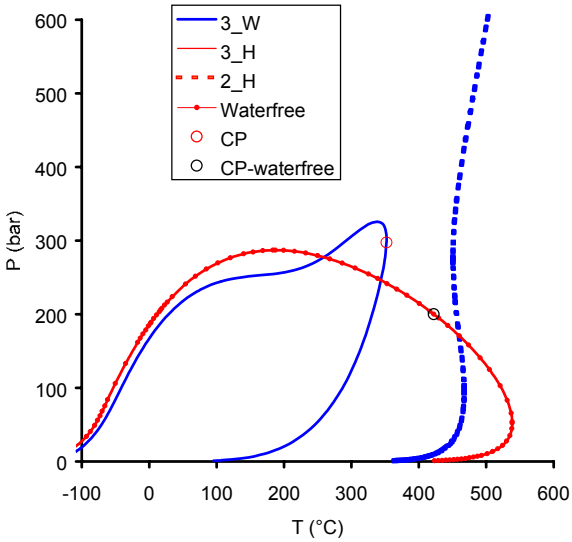


**Figure 7: Comparison of phase diagrams for Fluid C with and without aqueous phase present**

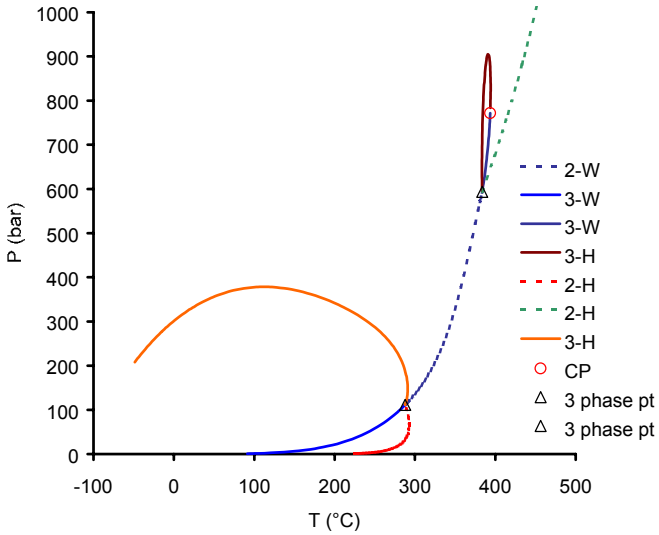


**Figure 8: Phase diagram for Fluid D with a 75% watercut.**